NEOPLASIA
www.neoplasia.com
Volume 22 Number 11 October 2020 pp. 590-603

The p53-inducible CLDN7 regulates colorectal tumorigenesis and has prognostic significance

Yichao Hou [a,1]; Lidan Hou [a,1]; Yu Liang [a,1]; Qingwei Zhang [b]; Xialu Hong [b]; Yu Wang [a]; Xin Huang [a]; Ting Zhong [a]; Wenjing Pang [a]; Ci Xu [a]; Liming Zhu [a]; Lei Li [a]; Jingyuan Fang [b,*]; Xiangjun Meng [a,*]

[a] Department of Gastroenterology, Shanghai Nineth People's Hospital, School of Medicine, Shanghai Jiao Tong University, Shanghai 200011, China; [b] Division of Gastroenterology and Hepatology, Key Laboratory Gastroenterology and Hepatology, Ministry of Health, State Key Laboratory for Oncogenes and Related Genes, Renji Hospital, School of Medicine, Shanghai Jiao Tong University, Shanghai Institute of Digestive Disease, Shanghai 200001, China

Abstract

Most colorectal cancer (CRC) are characterized by allele loss of the genes located on the short arm of chromosome 17 (17p13.1), including the tumor suppressor p53 gene. Although important, p53 is not the only driver of chromosome 17p loss. In this study, we explored the biological and prognostic significance of genes around p53 on 17p13.1 in CRC. The Cancer Genome Atlas (TCGA) were used to identify differentially expressed genes located between 1000 kb upstream and downstream of p53 gene. The function of CLDN7 was evaluated by both *in vitro* and *in vivo* experiments. Quantitative real-time PCR, western blot, and promoter luciferase activity, immunohistochemistry were used to explore the molecular drivers responsible for the development and progression of CRC. The results showed that CLDN7, located between 1000 kb upstream and downstream of p53 gene, were remarkably differentially expressed in tumor and normal tissues. CLDN7 expression also positively associated with p53 level in different stages of the adenoma-carcinoma sequence. Both *in vitro* and *in vivo* assays showed that CLDN7 inhibited cell proliferation in p53 wild type CRC cells, but had no effects on p53 mutant CRC cells. Mechanistically, p53 could bind to CLDN7 promoter region and regulate its expression. Clinically, high CLDN7 expression was negatively correlated with tumor size, invasion depth, lymphatic metastasis and AJCC III/IV stage, but was positively associated with favorable prognosis of CRC patients. Collectively, our work uncovers the tumor suppressive function for CLDN7 in a p53-dependent manner, which may mediate colorectal tumorigenesis induced by p53 deletion or mutation.

Neoplasia (2020) 22 590–603

Keywords: Colorectal cancer, p53, CLDN7, Deletion, Mutation

Introduction

Colorectal cancer (CRC) is one of the most commonly diagnosed cancer worldwide [1]. It is estimated that 145,600 patients will be diagnosed with CRC and that 51,020 patients will die from the disease in the United States in 2019 [2]. The development of CRC is a multistep process that is driven by the genetic or epigenetic inactivation of tumor suppressor genes and activation of oncogenes. Exploring the mechanisms underlying the growth and progression of CRC is essential for improving treatment.

Abbreviations: CRC, colorectal cancer, kb, kilobase, TCGA, The Cancer Genome Atlas, CLDN7, Claudin 7, WT, wild type, MT, mutant type, CCLE, Cancer Cell Line Encyclopedia, GEO, Gene Expression Omnibus, FDR, False Discovery Rate, GSEA, Gene set enrichment analysis, MF, molecular function, CC, cellular components, BP, biological processes, DOX, Doxorubicin, PFTα, pifithrin-α, ACTB, β-actin, qPCR, Quantitative PCR, SD, standard deviation, OS, overall survival, EFS, relapse free survival, CNV, copy number variation

* Corresponding authors at: Department of Gastroenterology, Shanghai Nineth People's Hospital, Shanghai Jiao Tong University, School of Medicine, 639 Zhi Zao Ju Road, Shanghai 200011, China (X. Meng). Division of Gastroenterology and Hepatology, Renji Hospital, School of Medicine, Shanghai Jiao-Tong University, Shanghai Institute of Digestive Disease, 145 Middle Shandong RD, Shanghai 200001, China (J. Fang).
e-mail addresses: jingyuanfang@sjtu.edu.cn (J. Fang), meng_xiangjun@yahoo.com (X. Meng).
[1] The authors contributed equally to this work.

https://doi.org/10.1016/j.neo.2020.09.001

Tumor suppressor p53, encoded by TP53 gene which is located on human chromosome 17p 13.1, is a critical tumor suppressor involved in maintaining genomic integrity [3]. Upon DNA damage, p53 is activated and triggers a transcriptional response that causes either cell arrest or apoptosis, ultimately reducing the risk of propagating mutations [4]. In recent years, increasing evidence shows that p53 can modulate autophagy, regulate metabolism, repress cellular plasticity, and facilitate ferroptosis [5–8]. Mutation and/or deletion of p53 gene that lead to the increase of tumorigenicity and invasiveness of cancer is observed in more than 50% of human cancers including CRC [9]. Mutations disabling the p53 gene frequently occur through a two-hit mechanism wherein one allele harbors a missense mutation and the other allele is deleted in a larger segmental human chromosome 17p deletion [10]. The most common p53 configuration involves a missense mutation together with a segmental 17p deletion [11]. In addition to p53, chromosome 17p encodes over 300 protein-coding genes that include other tumor suppressors functionally validated. Hence, chromosome 17p deletions can produce heterogeneity in the nature and number of p53-linked tumor suppressor genes subject to reduced dosage. In most cases, chromosome 17p deletions encompass all or most of the chromosome arm and are associated with poor prognosis in many tumors such as chronic lymphocytic leukemia [11], multiple myeloma [12] and acute myeloid leukemia [13]. Liu, Chen, and colleagues demonstrated that the loss of other genes in 17p13 region contributes multiple activities that act independently of p53 inactivation to drive tumorigenesis [10]. Moreover, deletions engineered to be syntenic to 17p13 drive more aggressive tumors than simple p53 deficiency in mice.

Collectively, it has become increasingly clear that both p53 mutations and chromosome 17p deletions contribute phenotypes to cancer that go beyond p53 loss. p53-regulated genes and interacted proteins form a huge network. It has been reported that positive and negative regulatory loops both upstream and downstream of p53 cooperate to finely tune its functions as a transcription factor. While p53 is known to transcriptionally activate numerous genes, it is still not clear how p53 target genes are activated and trigger tumorigenesis in CRC.

Here, we analyzed data on human colorectal carcinomas from the Cancer Genome Atlas (TCGA) collection to explore whether expression of genes located between 1000 kb upstream and downstream of p53 was regulated by altered activity of p53. We identified a p53-regulated gene named Claudin 7 (CLDN7), which is one of the most dominant claudins expressed in the intestine and is the main determinant of tight junction barrier function. Multiple databases and CRC tissue microarray showed that CLDN7 was remarkably down-regulated in CRC tissues and was associated with p53 expression, predicting satisfactory patient outcomes. In addition, upregulated CLDN7 dramatically contributed to the inhibition of wild type (WT) p53 cancer cell growth in *in vitro* and *in vivo* experiments. Mechanistically, WT p53 protein binds to the promoter region of CLDN7 and upregulates the expression of CLDN7. By contrast, mutant type (MT) p53 protein leads to an insignificant effect on the expression of CLDN7 in CRC cells. Moreover, CLDN7 could serve as a good prognostic indicator in p53 WT CRC patients but had no significantly prognostic prediction effect on p53 WT CRC patients, indicating that the effects of CLDN7 on CRC is closely related to p53 gene status. Overall, our study reveals that p53-inducible CLDN7 is a promising biomarker for prognostic prediction, and plays a tumor suppressor role in CRC in a p53-dependent manner.

Materials and methods

Data collection and data processing

The RNA-Seq data and additional patient information were downloaded from public TCGA (http://cancergenome.nih.gov/) CRC data repositories. The cancer cell line RNA-seq data of various types of cancer was downloaded from Broad Institute Cancer Cell Line Encyclopedia (CCLE, https://portals.broadinstitute.org/ccle). Count-based differential expression pipeline for mRNA-seq data were analyzed using R based package edge. The microarray data and additional patient information were downloaded from NCBIs Gene Expression Omnibus (GEO, http://www.ncbi.nlm.nih.gov/geo/). Data were preprocessed with `impute' package when needed. For finding differently expressed mRNAs, data were divided into two pattern including CRC and normal colorectal tissue. Different expressed mRNAs were acquired by `limma' package in R 3.2.1. Fold change $\geq$2 and False Discovery Rate (FDR) $\leq$0.01 were considered statistically significant.

Gene set enrichment analysis (GSEA) was performed to investigate the potential biological pathways involved in CRC pathogenesis via CLDN7. FDR of 0.01 was established as cut-off for the identification of biologically relevant genes. The gene sets showing with FDR more than 0.25 were considered enriched between the classes under comparison. The gene sets collection (c2.all.v4.0.symbols.gmt) from the Molecular Signatures Database–MsigDB (http://www.broad.mit.edu/gsea/msigdb/index.jsp) was used for the enrichment analysis.

Functional and pathway enrichment analysis

The gene ontology (GO) database has a large collection of gene annotation terms, allowing genome annotation using consistent terminology. GO enrichment analysis including molecular function (MF), cellular components (CC) and biological processes (BP), identified which GO terms were over or underrepresented within a given set of genes. GO analysis was conducted using the Database for Annotation, Visualization and Integrated Discovery (DAVID, Frederick, USA. https://david.ncifcrf.gov/), analysis tools for extracting meaningful biological information from multiple gene and protein collections.

Human tissue microarray analysis

Two human CRC tissue microarrays contained a total of 169 paired CRC and para-cancerous samples. Sections of CRC and normal tissue were stained with CLDN7 antibody (Abcam, USA). The tissue slides were evaluated by two independent investigators. Protein expression was evaluated based on intensity (the grade was measured on a scale of 0–3: 0, no staining; 1, weak staining; 2, moderate staining; 3, strong staining) and extent of staining (the percentage of positive tumor cells was measured on a scale of 0–4: 0, none; 1, 1–25%; 2, 26–50%; 3, 51–75%; 4, >75%). To obtain the final score, we multiplied the extent by grades of intensity staining. Then the samples were ranked by the final score. Protein expression was then ultimately stratified into high and low expression based on the median of the sample size.

Cell culture, reagents and transfection

The human CRC cell lines Lovo, HCT116 (p53WT), HCT116 (p53−/−) and HT29 (p53R273H) cells were obtained from ATCC (Manassas, VA, USA) and cultured in RPMI-1640 or Mycoy's 5a with 100 U/mL penicillin, 100 g/mL streptomycin and 10% fetal bovine serum. Doxorubicin (DOX) and pifithrin-α (PFTα) were obtained from Sigma-Aldrich. Expression plasmids for CLDN7 were generated by inserting synthesized cDNAs into pCDNA3.1 vector (GeneRay, Shanghai). Cells were seeded into six-well plates at 2×10^5 cells/well overnight and transfected with 1.5 μg plasmids using FuGene HD (Promega). SiRNAs specifically targeting p53 were purchased from GenePharma (Shanghai, China) using the following sequences: p53: siRNA-1, 5′-GUAAUCUA CUGGGACGGAATT-3′; siRNA-2, 5′-GAAGAAACCACUGGAUG

GATT-3′. Lovo or HCT116 cells were plated onto the six-well plates 24 h before transfection at 30% confluence, and the transfection was then performed with 50 nM siRNA using Dharma FECT 1 transfection reagent (Dharmacon, Lafayette, CO, USA) based on the manufacturer's instructions. A scrambled siRNA (GenePharma) was used as a control.

Quantitative real-time PCR analysis

Total RNA was isolated from cells 96 h after transfection by Trizol reagent (Invitrogen) and reverse transcription of total RNA was performed using a PrimeScript RT Reagent Kit (Perfect Real Time; Takara). Quantitative PCR (qPCR) was performed with SYBR Premix Ex Taq II (Takara) using an ABI Prism 7900HT Sequence Detection System (Applied Biosystems, USA), and the quantification was calculated using the 2_△△CT method and presented as fold change. β-Actin (ACTB) was used for normalization of the expression of each target gene, and the detailed primer sequences are shown in Suppl. Table 1.

Western blotting

Proteins were fractionated on a 10–12% SDS-polyacrylamide gel by electrophoresis and transferred onto polyvinylidene fluoride (PVDF, Bio-Rad, Hercules, CA) membranes. After blocking in 5% fat-free milk for 60 min, the membranes were incubated with primary antibodies against p53 (Santa Cruz), CLDN7 (Abcam), p21 (Cell Signaling), Occludin (Thermo Fisher), ZO1 (Thermo Fisher), E-cadherin (Cell Signaling), Cyclin D1 (Cell Signaling), Cyclin D3 (Cell Signaling), Cleaved caspase3 (Abcam), Cleaved caspase9 (Abcam) and Cleaved PARP (Abcam) at 4 ☒ overnight. After extensive washing, the membranes were incubated with secondary antibodies labeled with HRP (KangChen, China) and signals were detected using ECL Kit (Pierce Biotech, Rockford, IL). The images were then analyzed using ImageJ 1.43 software. Detection of β-actin (ACTB) was performed as an internal control. At least two independent experiments were performed in all experiments.

Cell viability assay

Cell viability was determined using a cell counting kit (CCK8) (Dojindo Laboratories, Japan). The transfected CRC cells were plated onto 96-well plates at 2000 cells/well, and cells were then incubated with CCK8 reagent (10 μL/well) for 2 hours at 37 °C after culture for 24, 48, 72, and 96 h. The optical densities were measured at 450 nm with a microplate reader (Molecular Devices Sunnyvale, CA, USA).

Colony formation assay

Briefly, the transfected CRC cells were plated into six-well plates at a density of 1000 cells/well and cultured for 9 days. Colonies were then fixed with 4% paraformaldehyde for 30 min and stained with 0.1% crystal violet for 10 min. Colonies with >100 cells were counted under an inverted microscope, and experiments were performed three separate times.

Apoptosis and cell cycle analysis

FITC-Annexin V apoptosis detection kit (Ebioscience, USA) was used for determination of cell apoptosis according to the manufacturer's protocol. After washing with PBS, the transfected CRC cells were resuspended in staining buffer, and 5 μl FITC-AnnexinV was added to 100 μl cell suspension. After incubation at room temperature for 20 min in darkness, cell preparation was subjected to flow cytometry analysis (Becton Dickinson, USA).

Cells were stained with propidium iodide (PI) for cell cycle analysis. Briefly, cells (1×10^6 cells/ml) were fixed with 70% ethanol for 24 h at 4 °C and incubated with PI for 30 min, after which cells were analyzed by flow cytometry (Becton Dickinson, USA).

Transwell assay

To perform transwell assay, we precoated the transwell chambers (8-μm pore size; Millipore, USA) with Matrigel (BD Biosciences, USA) that diluted in 1:4 proportion with serum-free medium. Cells were transfected with pCDNA3.1 and CLDN7 before 5×10^5 cells suspended in serum-free medium were seeded into the upper chamber, and the lower chamber was provided with medium containing 20% FBS as a chemoattractant. After 48 h incubating, cells that pass through the filter were fixed by 4% paraformaldehyde (Dingguo Biotechnologies, China) and stained by 0.1% crystal violet (BBI Life Sciences Corporation, China). The migrated cells could be counted by a microscope. Cell numbers in three randomly selected fields at 100× magnification were counted to compare the migration capacities of the cells between groups.

Cellular localization assays

CRC cells were fixed with methanol for 15 min, permeabilized in 0.2% Triton X-100 for 20 min and blocked with 5% BSA for 60 min at room temperature. After blocking, cells were incubated with primary antibodies (p53 or CLDN7) at 4 °C overnight. Then, cells were incubated with secondary antibody for 20 min at room temperature in a lucifugal chamber. Samples were washed with PBS for three times followed by treatment with DAPI. Samples were photographed using Zeiss LSM 510 laser confocal scanning microscopy.

Reporter gene constructs and luciferase assays

CLDN7 promoter regions were cloned into the Kpn I and Hind III sites of the promoter firefly luciferase reporter vector pGL3-Basic (Promega, Germany). Either p53 WT or p53 MT (p53R273H, p53R175H), and pGL3-CLDN7 (0.5 μg of each DNA/well) were co-transfected into HCT116 (p53WT) cells. pGL3-Basic served as the empty vector. Transfections were carried out using Lipofectamine 2000 (Invitrogen), according to the manufacturer's instructions. Twenty four hours after transfection, Firefly luciferase and Renilla luciferase activities were measured using the Dual Luciferase Reporter Assay System (Promega). The results were calculated as relative luciferase activity (Firefly luciferase/Renilla luciferase). The experiment was repeated at least three times.

Mouse xenograft model

Athymic male nu/nu mice aged 5 weeks were purchased and housed at Shanghai Model Organisms Research Center, and experiments were approved by the Research Ethics Committee. Subcutaneous implant model was established by subcutaneous injection of 5×10^6 cells stably expressing either lentivirus-Vector, or lentivirus-CLDN7, and tumor size was monitored with a callipers once every 2 days. Tumor volume was calculated by the following formula: volume = $0.5 \times \text{length} \times \text{width}^2$. After 20 days, mice were sacrificed for tumor harvest, and tumor weights were measured. The obtained tumors were subjected to IHC staining to evaluate the expression of Ki-67, cleaved caspase 3, p53 and CLDN7.

Statistical analysis

All statistical analyses were carried out using GraphPad Prism 8.0 or SPSS for Windows 17.0.1 software. Data from at least three independent

experiments performed in triplicates were presented as means þ standard deviation (SD). If data were with normal distribution and the variations were comparable between groups, the paired-sample t test or independent-sample t test was used for comparison between two groups. The comparisons among three or more groups were performed by One-Way ANOVA test if the variations between groups were comparable. Enumeration data were examined by Kappa test. The Chi-square test or Fisher Exact test was used to analyze clinicopathological data. Overall survival (OS) and relapse free survival (RFS) were evaluated using the Kaplan-Meier method and curves were compared with the log-rank test. Cox's proportional hazards regression model was applied to evaluate the prognostic factors by univariable and multivariable analyses. The correlation of the two genes was determined by Spearman correlation test. A value of $P < 0.05$ was set as the significant difference.

Results

Identification of differentially expressed genes around p53 on chromosome 17p13.1

To find out genes that may be regulated by p53 and participate in the development of CRC, we analyzed genes located between the upstream and downstream 1000 kb of p53 from Ensembl genome database and found a total of 157 transcripts (Suppl. Table 2). Then the expression of these transcripts was further investigated in normal colorectal and CRC tissues. Firstly, CRC data sets and corresponding clinical data were downloaded from the publicly available TCGA database. After removal of novel transcript, microRNA and small nucleolar RNA from 157 transcripts, 117 transcripts were analyzed in the present study (Suppl. Table 3, Suppl. Fig. 1A). Next, we generated a comparable heatmap and found that the expression of many genes was significantly different in CRC and adjacent normal tissues (Fig. 1A). Furthermore, functional and pathway enrichment analysis of the differentially expressed genes in this module were conducted using DAVID. GO term enrichment analysis demonstrated that genes were enriched in 28 pathways including apoptotic process (GO:0006915), positive regulation of angiogenesis (GO:0045766), and lipoxygenase pathway (GO:0019372) (Fig. 1B). Cell component analysis indicated that genes were significantly enriched in MLL1 complex, cytoplasm and membrane (Suppl. Fig. 1B). Molecular functional analysis demonstrated that the genes were primarily involved in oxidoreductase activity, hepoxilin A3 synthase activity and protein self-association (Suppl. Fig. 1C). Subsequently, 50 pairs of CRC and adjacent normal tissues from TCGA CRC cohort were further explored, and 40 genes were defined as significantly different between cancer and adjacently normal tissues with the adjusted p value of less than 0.05 with a fold change ≥ 2. We also screened the differentially expressed genes in four GEO databases, and CLDN7, NTN1, PITPNM3, TMEM88, TNFSF13, and VAMP2 were identified as differentially expressed genes in four GEO CRC cohorts using intersection calculation (Fig. 1C) (Table 1). The mRNA expression levels of the six genes in 50 CRC samples were significantly decreased compared with those in their paired normal tissues (Fig. 1D). Patients' OS and RFS analysis showed that CLDN7 was noted to be significantly associated with OS (Hazard ratio = 0.69, 95% CI = 0.48–0.99, $P = 0.0360$, Fig. 1E) and RFS (hazard ratio = 0.64, 95% CI = 0.43–0.95, $P = 0.0420$, Fig. 1F) in CRC patients, whereas other five genes have no significance in predicting the clinical outcome of these patients ($P > 0.05$). These data suggest that CLDN7, as a neighboring gene of p53, may play a role in the occurrence and progression of CRC.

CLDN7 expression associates with p53 activation and a better outcome in CRC

To clarify whether there was a relationship between CLDN7 and p53, we analyze the relationship between p53 and CLDN7 through different databases. Data from the Human Protein Atlas (Fig. 2A) suggested a positive association between the expression of CLDN7 and p53 in CRC tissues. Additionally, analysis of multiple datasets using a multiple experiment matrix revealed that mRNA level of six aforementioned genes (CLDN7, PITPNM3, TNFSF13, TMEM88, NTN1) were all positively correlated with p53 mRNA, among which CLDN7 mRNA expression significantly associated with p53 mRNA (Fig. 2B). Similarly, data from the TCGA dataset and the larger GEO CRC cohort confirmed positive association between the expression CLDN7 and p53 mRNA in CRC tissues (Fig. 2C). Moreover, CLDN7 expression also positively associated with p53 level in different stages of the adenoma-carcinoma sequence (Suppl. Table. 4). GSE39582 dataset revealed that the expression level of CLDN7 mRNA in p53 mutant group was significantly lower than that in p53 WT group (Fig. 2D). We further assessed the expression of CLDN7 in multiple CRC cell lines. Compared to CRC cell lines with MT p53, WT p53 CRC cell lines (RKO, Lovo and HCT116) tented to have higher expression level of CLDN7 (Suppl. Fig. 2A). Kaplan–Meier analysis was then applied to evaluate the OS and RFS of CRC patients with high or low expression of CLDN7 stratified by different p53 gene status (WT versus MT) (Fig. 2E). In p53 WT group, patients with low CLDN7 expression showed significantly shorter OS ($p = 0.236$) and RFS ($p = 0.0449$). However, CLDN7 expression exhibited no statistically significant value in predicting the OS ($p = 0.7639$) and RFS ($p = 0.5095$) of CRC patients in p53 MT group. These data suggested that the effect of CLDN7 on the prognosis of CRC was related to p53 gene status and might be more valuable in predicting the outcome of CRC patients with p53 WT.

CLDN7 is a p53-responsive gene

Altered gene expression can be associated with copy number variation (CNV) or a more complex pattern of dysregulation in gene expression control [14]. Methylation level of the promoter regions also affects the transcription rate [14]. To analyze the effect of DNA CNV and methylation on CLDN7 expression, we predicted CNV and DNA methylation of six differentially expressed genes identified in CRC above. The results revealed that compared with normal tissues, only 1.8% of CLDN7 in CRC underwent copy number variation, mainly in gene deletion, and there was no significant difference in DNA methylation (Suppl. Fig. 2B, C).

It has well been documented that p53 regulates target gene expression by binding to the p53 response elements in the promoter regions, thereby regulating cell proliferation, apoptosis, cell cycle and other cellular processes [15]. Therefore, it was reasonable to propose that p53 could be a transcription factor regulating CLDN7 expression. To test this hypothesis, we firstly observed the localization of p53 and CLDN7 in Lovo, HCT116 (p53WT) and HT29 (R273H) by immunofluorescence. It was shown that p53 was mainly located in the nucleus while CLDN7 predominantly distributed in the cytoplasm and cell membrane regardless of p53 status (Fig. 3A), suggesting that the endogenous CLDN7 and p53 proteins had no intracellular colocalization and physical interaction of CLDN7 and p53 was excluded. We therefore asked whether p53 could directly regulate CLDN7 expression. After knocking down or overexpressing p53 in Lovo and HCT116 cells (p53 WT), the expression level of CLDN7 also decreased or increased at mRNA and protein levels (Fig. 3B, C). We also investigated the typical genes including CLDN1, ZO1, E-cadherin, Occludin, and Jam1, which were involved in regulation of epithelium tight junction by western blot. Knockdown or overexpression of p53, the protein levels of these genes were rarely changed, indicating that p53 specifically modulate the expression of CLDN7 rather than the other tight junction-related genes (Suppl. Fig. 3A, 3B). Subsequently, we analyzed if p53 was regulated by CLDN7. p53 mRNA (Suppl. Fig. 3C)

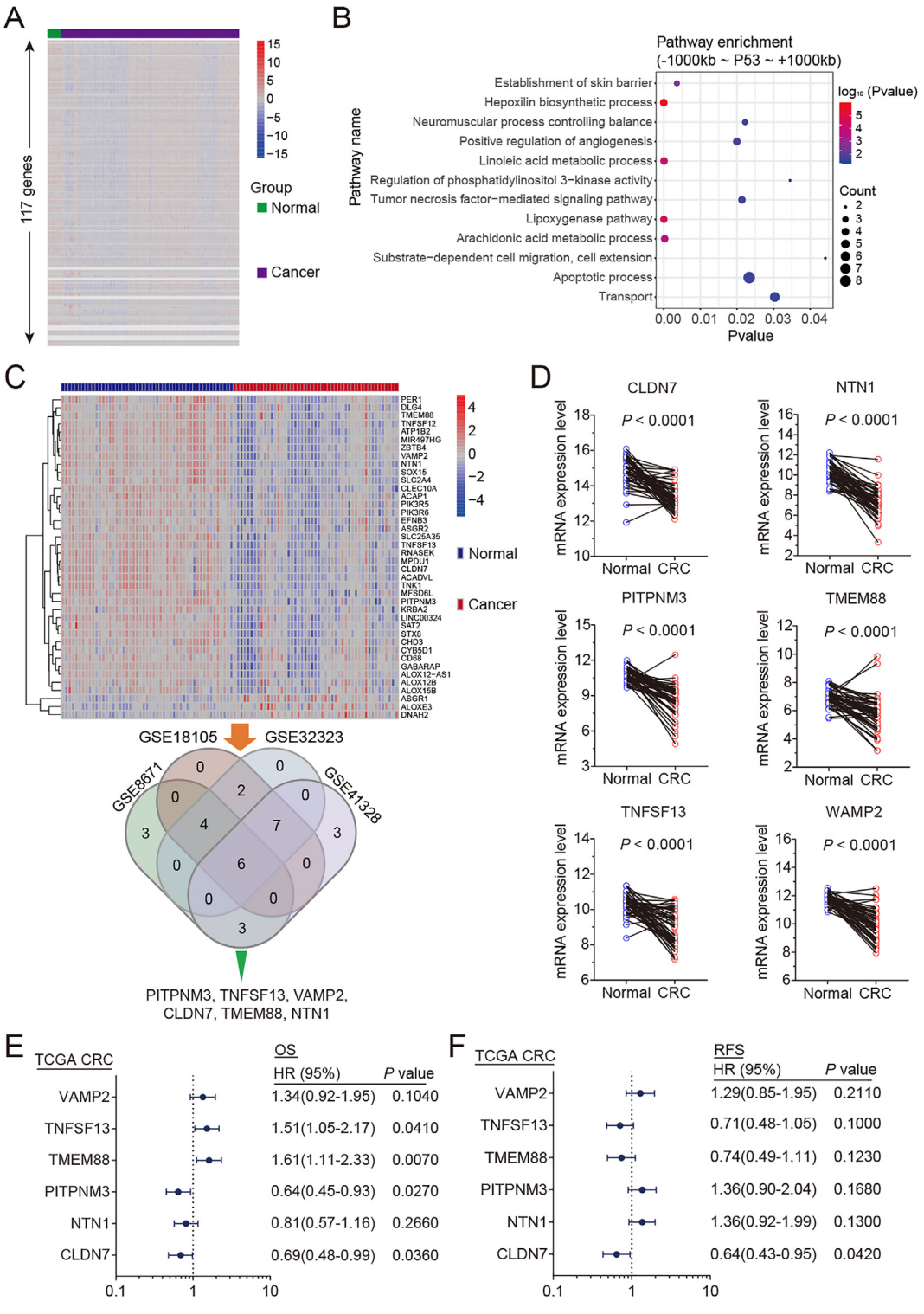

Fig. 1. Genetic analysis within 1000 kb upstream and downstream of p53. (A) Heatmap of genes located between 1000 kb upstream and downstream of p53 in adjacent normal and CRC tissues. 117 genes were defined as differentially expressed genes with $P < 0.05$ and fold change ≥ 2 in CRC TCGA database. Color represents gene transcripts above (red) or below (blue) the global median scaled to 15-fold upregulation or downregulation, respectively. (B) GO enrichment of genes located between 1000 kb upstream and downstream of p53 gene in CRC. Twelve pathway enrichment terms were displayed. Color indicates adjusted *p* value, and size indicates the number of enriched genes. Higher enrichment scores correlate with lower *P*-values, suggesting that the enrichment of the differentially expressed genes in a given pathway is significant. (C) Fifty pairs of CRC and adjacent normal tissues were analyzed. Venn diagram showed the down-regulated or up-regulated gene in four GEO colorectal cancer cohorts (GSE8671, GSE18105, GSE32323, and GSE42328). Six genes were identified as differentially expressed genes between cancer tissues/patients and normal tissues/patients in four cohorts. (D) Six differentially expressed genes in the same data set compared with paired-adjacent normal tissue using student's t-test. Plot represents the mRNA expression levels in 40 CRC samples and paired normal tissues ($P < 0.0001$). (E and F) Patients' overall survival (OS) and relapse free survival (RFS) of six differentially expressed genes were analyzed. The hazard ratio (HR) and 95% confident interval (CI) are plotted. All the bars correspond to 95% confidence intervals.

Table 1. Six genes significantly differentially expressed in normal and colorectal cancer tissues.

Gene name	Transcript stable ID	Chromosome	Transcript start (bp)	Transcript end (bp)	Strand	Gene description	Transcript type	LogFC (Normal/ CRC)	*P* Value
CLDN7	ENST00000360325	17	7E+06	7E+06	−1	Claudin 7	Protein coding	1.63	4.82E−33
NTN1	ENST00000173229	17	9E+06	9E+06	1	Netrin 1	Protein coding	3.52	4.27E−51
PITPNM3	ENST00000421306	17	6E+06	7E+06	−1	PITPNM family member 3	Protein coding	2.24	1.48E−28
TMEM88	ENST00000301599	17	8E+06	8E+06	1	Transmembrane protein 88	Protein coding	1.51	4.79E−21
TNFSF13	ENST00000483039	17	8E+06	8E+06	1	TNF superfamily member 13	Protein coding	1.64	1.18E−18
VAMP2	ENST00000316509	17	8E+06	8E+06	−1	Vesicle associated membrane protein 2	Protein coding	1.87	1.68E−34

and protein level (Suppl. Fig. 3D) did not significantly changed in CLDN7 overexpressed HCT116 cells. Dual luciferase reporter assay showed that no effect of CLDN7 on the transcriptional activity of p53 (Suppl. Fig. 3E), and p53 main target genes p21 $^{WAF1/Cip1}$, PUMA, GADD45A, BAX, FAS did not significantly upregulated or downregulated after overexpressing CLDN7 in HCT116 cells (Suppl. Fig. 3F). To further confirm that p53 was involved in mediating CLND7 expression, we treated HCT116 cells (p53WT) with the p53 stimulus DOX and pharmacological p53 transcriptional activity's inhibitor PFTα for various times, respectively. The results showed that mRNA and protein expression of p53 and CLDN7 was simultaneously increased after DOX stimulation (Fig. 3D). On the other hand, small-molecule inhibitor of p53 transcriptional activity reduced CLDN7 levels along with p21$^{WAF1/Cip1}$, especially at 36 hours (Fig. 3E). Furthermore, after overexpressing p53 WT and p53 MT (p53 R237H or p53 R175H) in HCT116 cells (p53WT) respectively, CLDN7 expression were significantly upregulated in p53 WT overexpressed cells at both the mRNA and protein levels, while did not obviously increase in p53 MT overexpressed cells (Fig. 3F). We identified binding sites for p53 in CLDN7 transcripts in silico promoter prediction (Suppl. Table 5). To test whether p53 binds to CLDN7 promoter, dual luciferase reporter assay was performed. HCT116 cells (p53WT) were transfected with luciferase reporter pGL3-Basic or pGL3-CLDN7 and luciferase activity was measured in cells with different p53 gene status. The results showed that the fluorescence intensity of the p53 WT group was significantly higher than p53 MT groups, suggesting that p53 WT but not p53 MT binds directly to the promoter region of CLDN7 (Fig. 3G). Taken together, our findings suggested that CLDN7 was positively regulated by p53 WT, which functions as a transcription factor and regulates the expression of CLDN7 by binding to its promoter region.

CLDN7 functions as a tumor suppressor in CRC depending on p53 status

To clarify whether CLDN7 played a role in CRC tumorigenesis, the gene expression profiles in TCGA CRC cohort with high or low expression of CLDN7 were performed by GSEA analysis. GSEA revealed that the gene sets, including GO_NEGATIVE_REGULATION_OF_EPITHELIAL_CELL_PROLIFERATION, GO_NEGATIVE_REGULATION_OF_CELL_CYCLE, ALCALA_APOPTOSIS and KEGG_P53_SIGNALING_PATHWAY, were positively correlated with high CLDN7 group (Fig. 4A–D). For further understanding the biological pathways involved in CRC pathogenesis, the gene sets were visualized as interaction networks with the Cytoscape based on the median of CLDN7 expression levels. The results showed that the gene signatures of cell proliferation, cell cycle, p53 pathway signaling, metabolism of proteins, and pathways in cancer were enriched in patients with high CLDN7 expression, but not in patients with low CLDN7 expression (Fig. 4E). These data implied that CLDN7 may be related to p53 and is an important modulator in CRC tumorigenesis.

Subsequently, *in vitro* assays were performed to verify the previous findings. Two cell lines with high CLDN7 protein levels, Lovo and HCT116 (p53 WT), and p53 MT cell line HT29 cells as well as p53-deficient cell line HCT116 (p53−/−) cells with low CLDN7 protein expression, were selected for functional analysis (Suppl. Fig. 2A). CLDN7 was overexpressed in Lovo, HCT116 (p53WT), HCT116 (p53−/−) and HT29 (p53R273H) cells, respectively. Cell proliferation assay showed that CLDN7 overexpression led to marked inhibition of cell proliferation in Lovo and HCT116 (p53WT) cell lines, whereas had no significant effect on the proliferation of HCT116 (p53−/−) and HT29 (p53R273H) cells (Fig. 5A). Colony formation assays showed similar results. Compared with CLDN7 overexpressed HCT116 (p53−/−) and HT29 (p53R273H) cells, it was shown that approximately two-fold less colonies were found in CLDN7 overexpressed Lovo, HCT116 (p53WT) cells (Fig. 5B). Subsequently, flow cytometry was performed to determine the effect of CLDN7 on cell apoptosis and cycle. As shown in Fig. 5C, upregulation of CLDN7 significantly increased the proportion of apoptotic cells in Lovo and HCT116 (p53WT) cell lines compared with that in the control groups. However, no significant differences were identified in HCT116 (p53−/−) and HT29 (p53R273H) cells between CLDN7 and control group (Suppl. Fig. 4A). In addition, upregulation of CLDN7 induced G0/G1 phase arrest of the cell cycle in Lovo and HCT116 (p53WT) cell lines but not HCT116 (p53−/−) and HT29 (p53R273H) cells (Fig. 5D, Suppl. Fig. 4B). The promoting effect of CLDN7 on cell cycle arrest was confirmed by the decreased protein expression of two master G1-S checkpoint regulators (cyclin D1 and cyclin D3). Furthermore, CLDN7-induced promotion of apoptosis was confirmed by elevated expression of key apoptosis markers (cleaved forms of caspase3, caspase9 and PARP). However, no significant differences were identified in HCT116 (p53−/−) and HT29 (p53R273H) cells between two groups (Fig. 5E). Additionally, overexpression of CLDN7 had no effect on main tight junction-related protein (Suppl. Fig. 4C). These results revealed that CLDN7 had no effect on p53 MT CRC cells, and CLDN7 might inhibit cell growth by regulating cell cycle progression and apoptosis independent on affecting epithelial tight junction in p53 WT cells. Therefore, a wild-type p53 is required for CLDN7 to function as a tumor suppressor in CRC cells. We also examined the effects of CLDN7 on CRC cell invasion and metastasis. In the transwell assay, we showed that ectopic expression of CLDN7 significantly decreased the migration abilities in Lovo and HCT116 (p53 WT) cells, and greatly suppressed invasiveness of both cells (Suppl. Fig. 4D).

Next, we examined the *in vivo* roles of CLDN7 in Lovo, HCT116 (p53 WT), HCT116 (p53−/−) and HT29 (p53R273H) cells. CRC cell lines stably expressing CLDN7 or cells harboring the control vector were

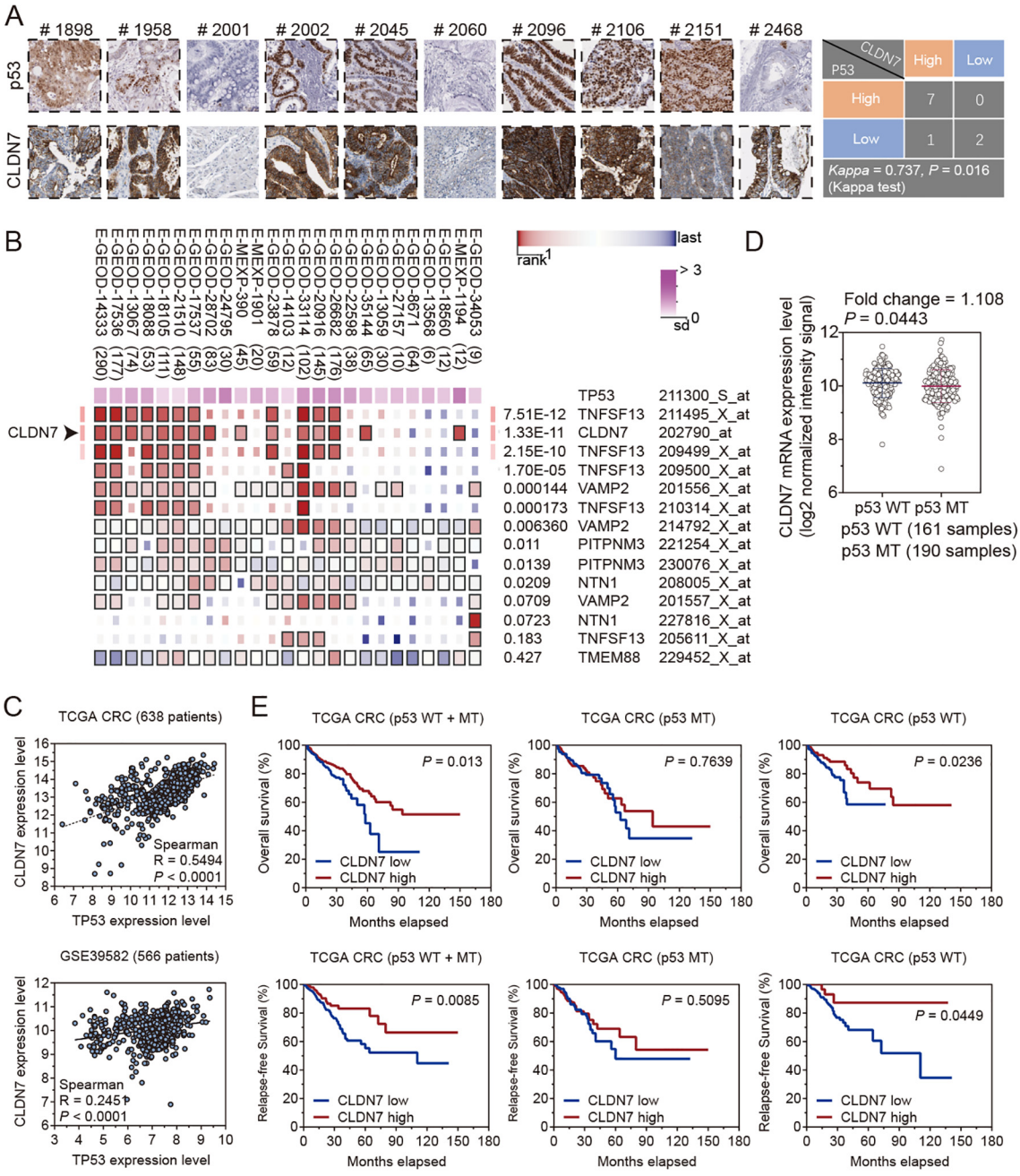

Fig. 2. p53 is related to CLDN7 expression and affects the role of CLDN7 in CRC patients' prognosis in the database. (A) Representative images of CLDN7 and p53 in CRC tissues detected by IHC were shown, respectively. The relationship between CLDN7 and p53 expression was statistically analyzed by Kappa test. (B) Correlation between six differentially expressed genes (CLDN7, PITPNM3, TNFSF13, TMEM88, NTN1) mRNAs and p53 mRNA used by multiple experiment matrix (MEM). (C) Spearman correlation analysis for CLDN7 in CRC versus p53. Plotted data are $\log^2$ mRNA expression from TCGA and GSE39582. (D) CRC patients with WT p53 (blue) and MT p53 (red) from GSE39582 were analyzed for CLDN7 mRNA expression. The horizontal line represents the mean values. *P*-values were calculated using paired Student's *t*-tests. (E) Kaplan–Meier analysis for the OS and RFS of CRC patients with different p53 gene status separated into two groups by optimum cut-off value for the CLDN7 expression. *P* values were calculated by a log-rank test.

subcutaneously inoculated into nude mice for further investigation of the tumorigenicity of CLDN7. The tumor size formed by Lovo and HCT116 (p53 WT) cells stably expressing CLDN7 was significantly smaller than that formed by the control cells, with a significant slower growth rate of the tumor xenografts (Fig. 5F). CLDN7 also significantly inhibited tumor growth, as reflected by the tumor weight compared with those of tumors derived from the vector control cells (Fig. 5G). Nevertheless, HCT116 (p53−/−) and HT29 (p53R273H) cells stably expressing CLDN7 showed no obvious differences in tumor size, tumor weight and tumor xenografts growth compared with the controls (Suppl. Fig. 4E, F). Moreover, immunohistochemical analysis using tumor proliferation marker Ki-67 antibody and apoptosis marker cleaved caspase 3 antibody were employed to evaluate the proliferation of the tumor xenografts. In concordance with the *in vitro* findings, fewer proliferating cells were detected in

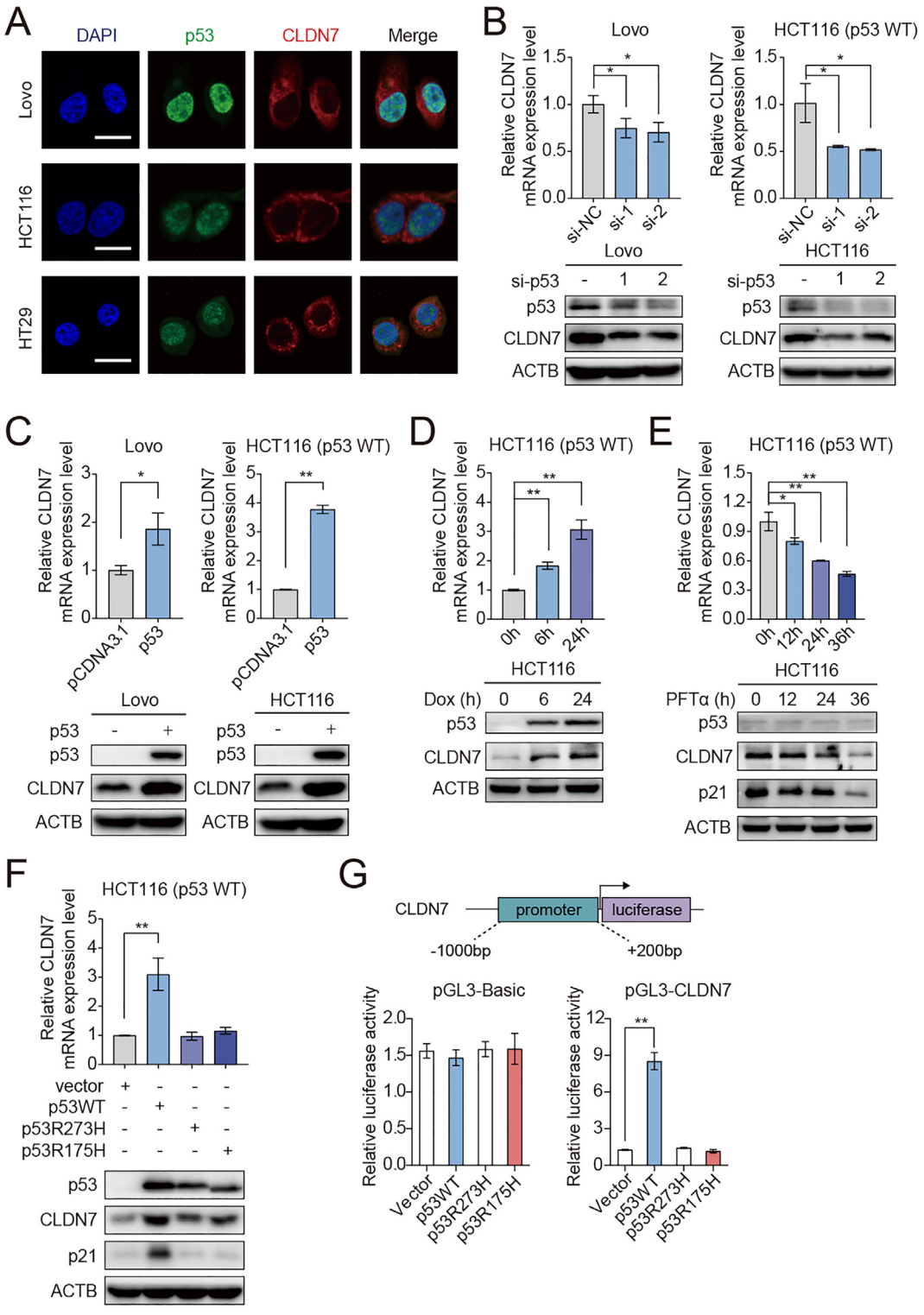

Fig. 3. p53 binds to CLDN7 gene promoter and regulates its expression. (A) Localization of p53 and CLDN7 in Lovo cells, HCT116 cells (p53 WT) and HT29 cells (R273H) was observed under confocal microscopy. Green fluorescence signals are from p53, and red fluorescence indicates CLDN7. Scale bars indicate 5 mm. (B and C) After knockdown or overexpression of p53 in Lovo and HCT116 cells (p53 WT), mRNA and protein expression of CLDN7 was detected by PCR and western blot analysis. (D and E) HCT116 cells (p53 WT) were treated with p53 stimulator DOX or a pharmacological inhibitor (PFTα) of p53 transcriptional activity for different times. mRNA and protein expression of p53 and CLDN7 was measured, respectively. (F) p53 WT and p53 MT (p53R237H or p53R175H) were overexpressed in HCT116 cells (p53WT) respectively, and then CLDN7 expression was detected by PCR and western blot analysis. $p21^{WAF1/Cip1}$ was served as positive control. (G) Firefly luciferase and Renilla luciferase expression vectors were used for the dual luciferase reporter system. HCT116 cells (p53WT) were transfected with luciferase reporter pGL3-Basic or pGL3-CLDN7 and luciferase activity was measured in cells with different p53 gene status. The results were calculated as relative luciferase activity (Firefly luciferase/Renilla luciferase). The data are the means þ SD of three independent experiments, $^{*}P < 0.05$; $^{**}P < 0.01$.

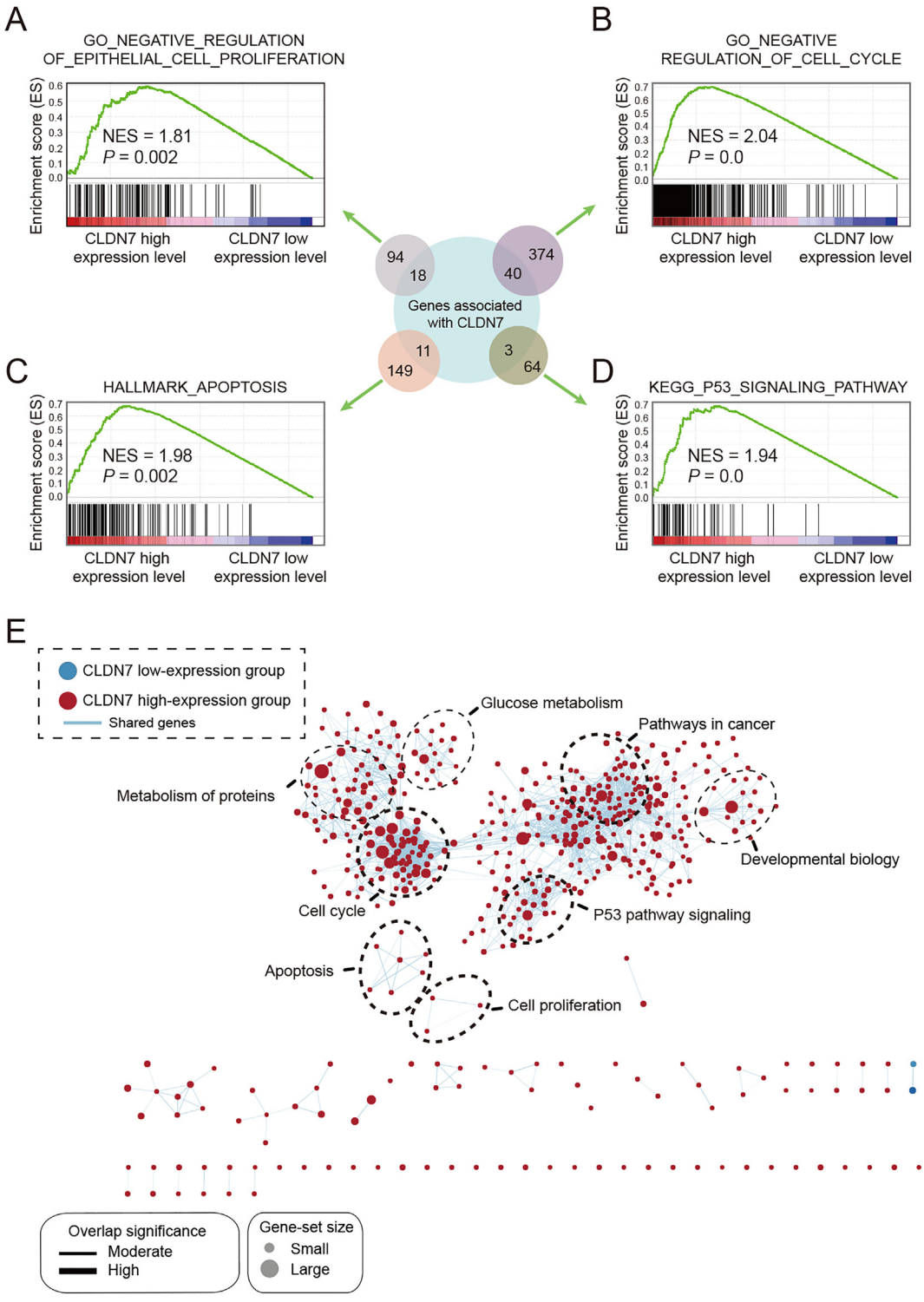

Fig. 4. Correlation between tumorigenic gene sets and CLDN7 expression levels is assessed via GSEA used by TCGA CRC cohort. (A–D) overview of GSEA used to identify the differential gene profiles between CLDN7 high expression and CLDN7 low expression group. Three typical cancer-related pathways and p53 signaling pathways were displayed. E. TCGA comparison between patients with CLDN7 high expression (red) and CLDN7 low expression (blue). Median split, $n = 319$ (TCGA CRC). Distinct pathways and biological processes were delineated between the two patient groups. Cytoscape and Enrichment map were used for visualization of the TCGA results (1% FDR; $P = 0.005$). Each node represents an enriched gene set, and they were grouped and annotated by the similarity according to related gene sets.

xenografts formed by Lovo and HCT116 (p53 WT) CLDN7 overexpressing cells compared with those in xenografts formed by control cells (Fig. 5H). More apoptotic cells were detected in xenografts formed by Lovo and HCT116 (p53 WT) CLDN7 overexpressing cells compared with those in xenografts formed by control cells (Fig. 5H). However, no significantly differences were found between control and HCT116

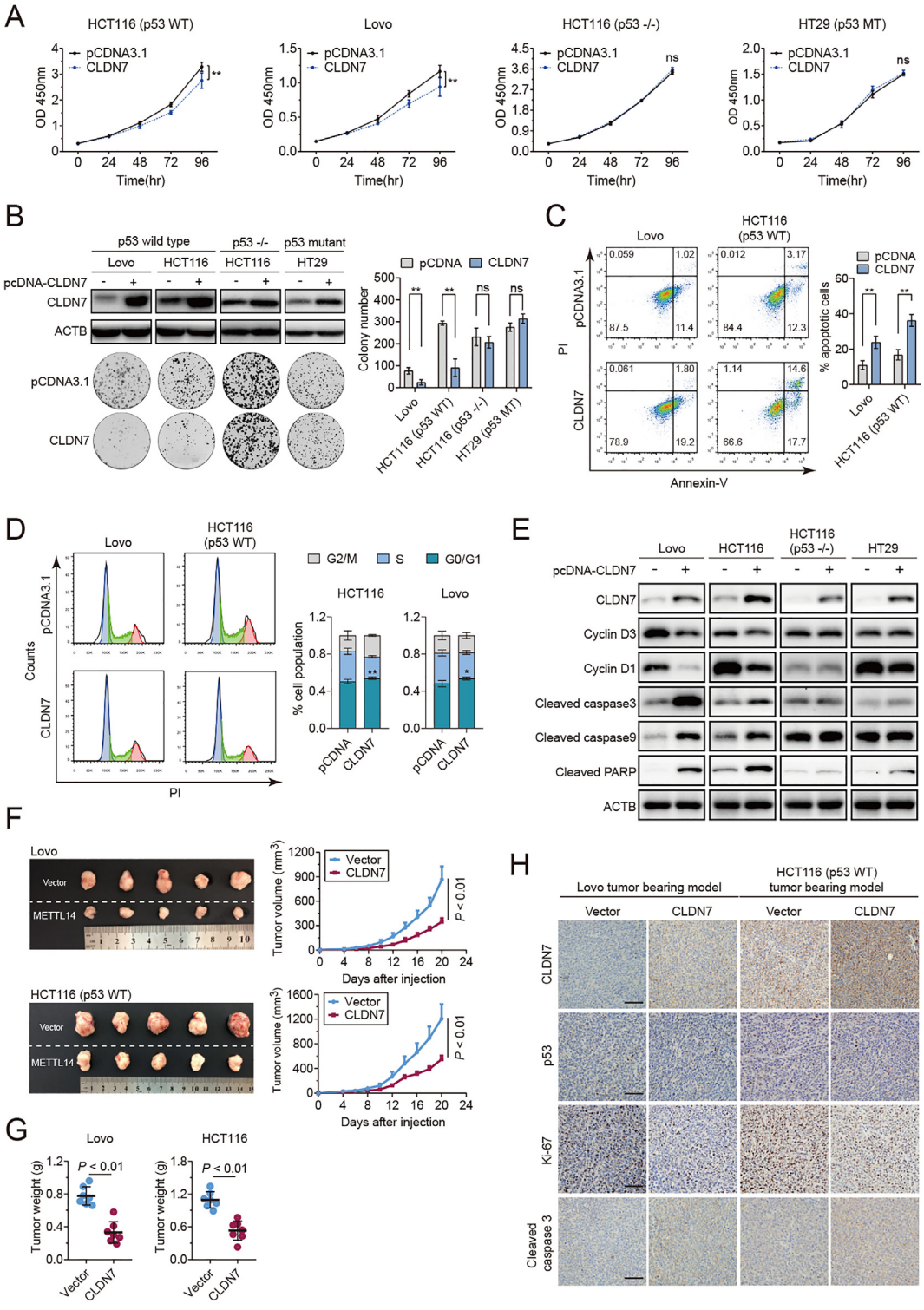

Fig. 5. CLDN7 plays a tumor suppressor role in CRC cells in a p53-dependent manner. (A) CCK8 assay was performed to determine cell viability. (B) CLDN7 expression of CRC with different p53 status was determined by western blotting and cell colony formation capacity was detected and qualified. (C and D) Cell apoptosis and cell cycle were determined by flow cytometric analysis. (E) The expression levels of cell cycle-related protein cyclin D1, cyclin D3, and apoptosis-related protein cleaved caspases 3, 9 and PARP were determined by western blotting in CRC cells with CLDN7 or pCDNA. (F and G) Lovo and HCT116 (p53WT) cells stably expressing the control vector or CLDN7 were injected subcutaneously into nude mice ($n = 7$ for each group). Tumor volumes were measured at the indicated time points and the mean tumor volumes were calculated. Data are presented as the mean þ SD. At the end of experiment, tumors from two groups were dissected, photographed, and weighed. H. Sections of tumor xenografts from CLDN7 overexpressing p53 WT CRC cells subcutaneously injected nude mice were stained with CLDN7, p53, ki-67 and cleaved caspase 3 antibodies by immunohistochemical (IHC) (scale bars = 100 μm). The data are the means þ SD of three independent experiments, $^{*}P < 0.05$; $^{**}P < 0.01$.

(p53−/−) and HT29 (p53R273H) CLDN7 group (Suppl. Fig. 4G). In summary, our *in vivo* results further support the tumor-suppressing role of CLDN7 in CRC dependent on p53 gene status.

CLDN7 downregulation is correlated with poor clinical outcomes in CRC patients

To further verify the relationship between CLDN7 and CRC, we examined CLDN7 mRNA expression in different type of cancer cell lines from Broad Institute Cancer Cell Line Encyclopedia (CCLE). The results showed that CLDN7 mRNA expression was highly expressed in 63 CRC cells (Suppl. Fig. 5A). We next investigated whether CLDN7 expression was altered in a variety of cancers. CLND7 varied in its expression in different cancers, but it was down-regulated exclusively in CRC (Suppl. Fig. 5B). The data were particularly striking for CRC, wherein the CLDN7 mRNAs were much lower in abundance in CRC tissues than in paired-adjacent normal tissues in the vast majority of GEO colorectal cancer cohorts (Suppl. Table 6), and colon polyp and adenoma in seven colorectal polyp cohorts (Suppl. Table 7). Several representative database analyses (GSE39582, GSE41258, GSE68468, and GSE37364) were shown in Suppl. Fig. 5C. Furthermore, clinical outcomes of the CRC patients with high or low CLDN7 were further analyzed. The Kaplan–Meier analyses showed that low level of CLDN7 was significantly correlated with a poor prognosis in CRC patients (Suppl. Fig. 5D). Collectively, all these data provide evidence that decreased expression of CLDN7 may contribute to CRC tumorigenesis, indicating its tumor suppressor function in CRC.

To validate the clinical significance of CLDN7 in CRC patients, we detected and compared CLDN7 expression by human CRC tissue microarray with immunohistochemical (IHC) staining, which consisted of two cohorts, containing a total of 169 paired CRC and normal tissue samples. Representative images of IHC staining for CLDN7 were shown in Fig. 6A and Suppl. Fig. 6A. The expression levels of CLDN7 were measured semi-quantitatively by multiplying the staining proportion score and the intensity score. Consistent with our previous findings, CLDN7 was significantly down-regulated in CRC tissues compared with that in normal non-tumor colon tissues in cohort 1 ($n = 90$, $p < 0.001$) and cohort 2 ($n = 79$, $p < 0.001$; Fig. 6B). We next evaluated and compared CLDN7 expression with different clinicopathologic features in cohort 1 (Fig. 6C). We found that high CLDN7 expression was negatively correlated with tumor size, invasion depth, lymphatic metastasis and AJCC III/IV stage. In cohort 2, high CLDN7 expression was negatively correlated with serosa penetration, invasion depth, lymphatic metastasis and AJCC III/IV stage (Suppl. Fig. 6B). Based on CLDN7 IHC staining intensity, the patients were classified into CLND7-low expression group and CLND7-high expression group. The Kaplan–Meier survival analysis revealed that patients with low CLDN7 expression level were significantly correlated with worse overall survival compared with those with high CLDN7 expression in cohort 1 ($n = 90$, HR = 0.36, $p = 0.02$; Fig. 6D) and cohort 2 ($n = 101$, HR = 0.26, $p < 0.001$; Fig. 6E). To accomplish a prognostic evaluation, we analyzed the clinical data of the CRC patients. Univariate analysis revealed that histological grade, lymph node metastasis and CLDN7 expression were significantly correlated with OS in CRC patients (Suppl. Fig. 6C, D). Subsequent multivariate analysis showed CLDN7 was negatively correlated with the OS of CRC patients and was an independent predictor of CRC prognosis (Fig. 6F, G, Cohort 1, HR = 0.36, $p = 0.004$; Cohort 2, HR = 0.32, $p < 0.001$).

Discussion

As a key molecular node, p53 consists of a very complicated gene network along with its downstream target genes, and activation of p53 by various cellular signals leads to the maintenance of genetic stability. Even though more and more p53 target genes are identified, it is believed that the majority fraction of p53 target genes has yet to be identified. Identifying important target of p53 in CRC not only helps us understand p53 gene regulatory network but also promotes an in-depth understanding of CRC tumorigenesis, thereby leading to the development of therapeutic applications in CRC.

In this study, the genes located between the upstream and downstream 1000 kb of p53 were analyzed by bioinformatics methods. 117 genes were differentially expressed in CRC tissues, and most of them were downregulated, suggesting that they may function as tumor-suppressive genes. Subsequently, GO enrichment analysis showed that differentially expressed genes were involved in multiple tumor-associated pathways such as apoptotic process. These findings inspired us to further analyze genes associated with the occurrence and development of CRC. Thus, we performed paired analysis in the TCGA database and then intersected with four GEO databases and six differentially expressed genes were eventually identified, but only CLDN7 was closely related to the clinical prognosis of CRC. Therefore, this study focused on the relationship between CLDN7 and development of CRC.

CLDN7, one of the claudins family members, is an important constituent of tight junctions in epithelial cells. Disruption of tight junction complexes is associated with multiple human diseases, including cancers [16]. Previous study has shown that CLDN7 is downregulated in a variety of cancers, such as CRC, head and neck cancer, and esophagus cancer, but upregulated in other cancers, such as ovarian cancer and gastric cancer [17,18], which was consistent with our Oncomine data analysis. In normal intestinal epithelium, the expression of CLDN7 is high and one of the important mechanisms of CRC progression may be the weakening of the endothelial barrier function in response to injury. It has been reported that CLDN7 expression induces mesenchymal to epithelial transformation to inhibit CRC tumorigenesis [19,20]. Moreover, CLDN7 may suppress the proliferation and migration of CRC cells by interacting with integrin β1 [21]. One study found that CLND7 was greatly decreased in human colon cancer tissues and indirectly regulated the integrin/FAK signaling pathway in colon cancer tissue [22]. In addition, CLDN7 deficient mice result in severe intestinal defects, including severe intestinal inflammation, altered epithelial cell homeostasis and even neonatal death [23,24]. Knight et al. [25] uncovered that loss of tumor suppressor gene p53 combined with the expression of a receptor tyrosine kinase in mammary gland of a murine model, synergize to promote tumors with pathological and molecular features of CLDN-low breast cancer. Although previous studies have shown that CLDN7 expression is reduced in CRC and inhibits the development of CRC, it is still unclear whether the tumor suppressor effect of CLDN7 in CRC is associated with p53. To explore the relationship between CLDN7 and p53, we analyzed p53 and CLDN7 co-expression analysis through multiple databases, and the results showed that p53 was significantly correlated with CLDN7 at protein and mRNA levels. Importantly, CLDN7 expression level was significantly different in p53 WT and p53 MT CRC tissues, and high CLDN7 expression predicted a good clinical outcome in CRC patients with p53 WT but not p53 MT. The results indicated that p53 is corelated to CLDN7 expression and affects the role of CLDN7 in CRC patients.

Previous study showed that DNA CNVs or/and DNA promoter hypermethylation can lead directly to deregulation of gene expression [26]. It is estimated that CNVs occur in about 9.5% of the human reference genome [27]. CNVs modulate gene expression by a variety of mechanisms, including simple gene dosage effects, duplication or deletion of the regulatory regions of the target genes, or changes in physical proximity of genes and response elements [28]. It was reported that deletion of EFNB3 gene and CpG hypermethylation of EFNB3 promoter with 63.2% GC content are closely linked to p53 tumor suppressor gene on human

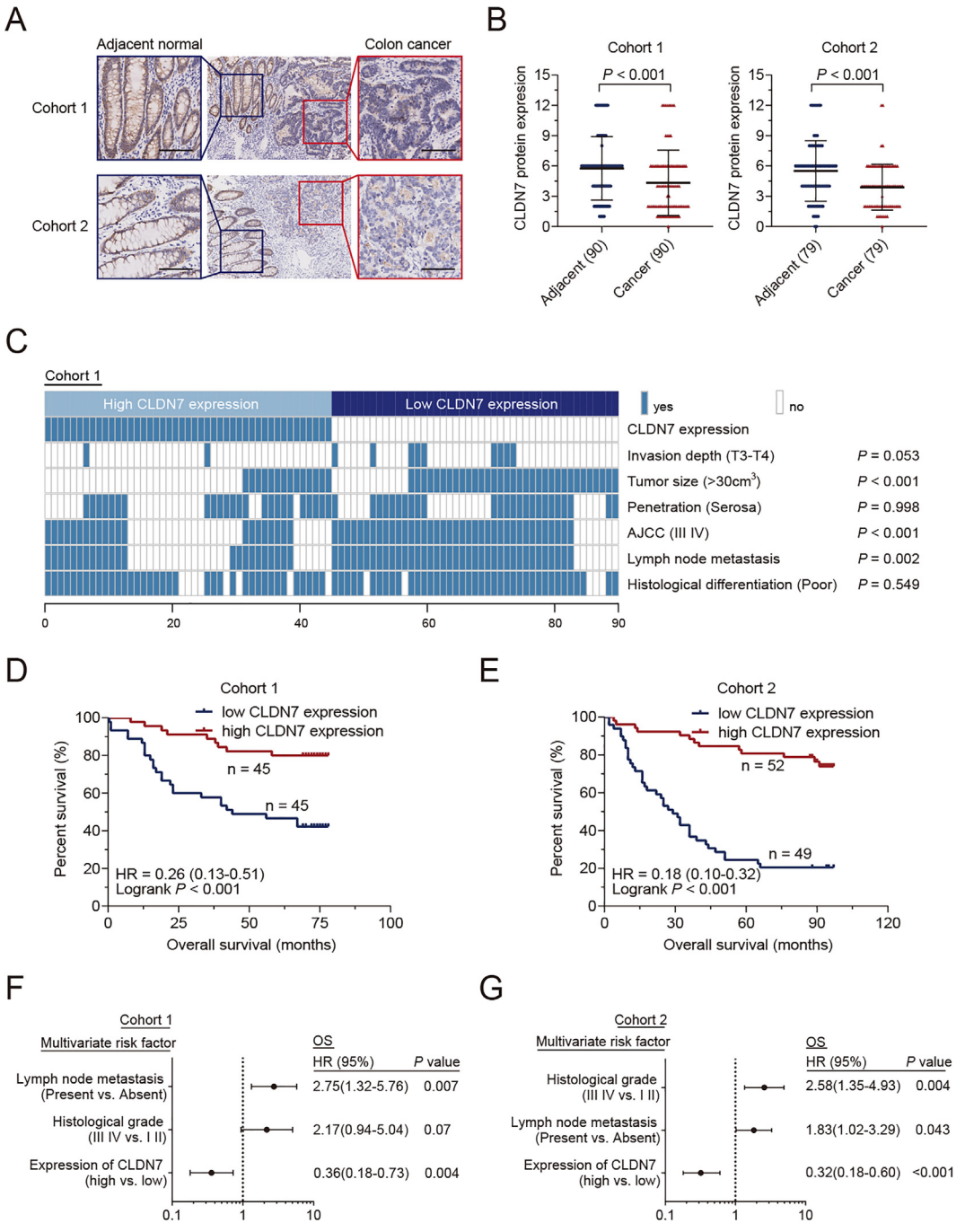

Fig. 6. Low CLDN7 expression is associated with poor prognosis in human CRC tissue microarray cohorts. (A) Representative photographs of CLDN7 IHC staining patterns with CRC and adjacent normal tissues in two tissue microarray cohorts were shown. Scale bar, 20 μm. (B) CLDN7 expression in CRC and paired adjacent non-tumor tissues was analyzed. (C) The heatmap illustrating the association of different clinical characters with CLDN7 high and low-expression tumors in cohort 1. (D and E) Kaplan–Meier analysis of the OS rate in CRC patients with different CLDN7 expression levels in two cohorts. (F and G) Multivariate regression analysis was performed to analyze the correlation of clinic-pathological features (Histological grade, lymph node metastasis) and CLDN7 expression with OS in two cohorts. All the bars correspond to 95% confidence intervals.

chromosome 17p13.1, which might cause the relatively infrequent expression of EFNB3 mRNA in CRC [29]. Therefore, CLDN7 CNVs were first investigated to reveal the underlying mechanism which may lead to CLDN7 downregulation in CRC. The analysis revealed that only 1.8% of CLDN7 underwent CNVs, indicating that the down-regulation of CLDN7 expression was not mainly due to genetic alteration. In addition, it was reported that DNA hypermethylation in the promoter of CLDN7 can result in down-regulation of CLDN7 expression. Hypermethylation at the CLDN7 promoter occurred in 20% of CRCs with low CLDN7 expression and the resultant decreased CLDN7 expression plays a critical role in CRC progression [30]. Similarly, hypermethylation of CLDN7 promoter is responsible for the down-regulation in breast cancer cell lines [31,32], which is similar to the report on human clear cell renal cell carcinoma [33].

Herein, we found that there was no significant difference in CLDN7 DNA methylation between CRC and normal patients ($P = 0.68$), suggest-

ing the mechanism of downregulation of CLDN7 in CRC could not be ascribed to promoter hypermethylation. After excluding the effect of CNVs and DNA methylation on CLDN7 expression levels, we studied the effect of p53 on the expression level of CLDN7. These findings prompted us to further investigate the underlying regulation mechanism of p53 on CLDN7. We observed that upon overexpressing p53 or stimulating p53 expression by DOX in CRC cells, expression of CLDN7 mRNA and protein was obviously up-regulated, and vice versa. However, CLDN7 mRNA and protein expression was not significantly up-regulated in CRC cells overexpressing p53 MT. Taken together, we believed that p53 may play an important role in regulating CLDN7 expression. Identifying the underlying interactive regulation mechanism of p53 and CLDN7 may be of high relevance for cancer prevention and treatment. Cellular localization experiment revealed that p53 did not colocalize with CLDN7, indicating that p53 did not affect CLDN7 expression by directly interacting with CLDN7 protein. As a transcription factor, binding to the gene promoter is the main mechanism by which p53 regulates target gene expression [34]. Therefore, we hypothesized that p53 might bind to CLDN7 promoter region to regulate its expression. Thus, we conducted luciferase reporter assay to confirm our conjecture. The results showed that p53 WT but not p53 MT could directly bind to CLDN7 promoter region. Further study revealed that p53 target gene promoter did not respond to CLDN7, and the mRNA expression levels of several p53 target gene did not change significantly in CLDN7 over-expressing CRC cells, indicating that CLDN7 had no feedback regulation on p53 expression.

Moreover, different gene expression profiles in CRC patients between low- and high-CLDN7 expression groups were further evaluated by GSEA, and multiple regulated networks of genes that were either upregulated or downregulated were identified, including those in the regulation of cell proliferation, cell cycle, apoptosis, and p53 pathway signaling. To verify the results of GSEA, *in vitro* and *in vivo* assays were performed, which demonstrated that CLDN7 overexpression significantly inhibited cell proliferation in p53 WT cells but not p53 MT cells, suggesting that CLDN7 functions as a tumor suppressor in CRC depending on p53 gene status. Multiple databases and human CRC tissue microarray analyses further revealed that CLDN7 was decreased in CRC cells and low CLDN7 expression was significantly associated with patients' poor OS, which was consistent with previous reports.

Overall, we first discovered that CLDN7, located at downstream of p53 on 17p13.1, was regulated by WT p53 through binding to its promotor region in CRC. Once p53 is mutated or deleted, the tumor suppressive function of CLDN7 disappears. These findings suggest that CLDN7 plays a tumor suppressor role via p53-dependent manner in CRC and p53-dependent downregulation of CLDN7 may mediate colorectal tumorigenesis induced by 17p13.1 deletion. Given there is only a 1.11 fold change in CLDN7 mRNA expression in p53 WT vs p53 MT CRC. Further studies are required to test whether CLDN7 has a p53-dependent role in anticancer properties of other tumors and to determine the differential expression of CLDN7 through more large survey sample with p53 WT and MT CRC tissues. In, conclusion, our study promotes an in-depth understanding of CRC tumorigenesis, which may lead to the development of therapeutic applications in CRC.

Acknowledgement

The authors are grateful to all the people who participated in the study.

Funding

This project was supported by grants from the National Natural Science Foundation of China (Grant No.81872419 and 81802304). This work was also supported in part by grants from the Interdisciplinary Program of Shanghai Jiao Tong University (ZH2018QNA01), and Shanghai Sailing Program (19YF1426900).

Conflict of interest

The authors declare that they have no potential conflicts of interest.

Authors contributions

YH, LH and YL participated in the design and performance of the study. QZ, XH, YH, LH, YL, YW, XH, TZ, WP, CX, LZ, LL participated in analysis and interpretation. XM conceived and supervised the study. XM designed or/and supervised this project and revised the manuscript. The author (s) read and approved the final manuscript.

Data accessibility

The datasets supporting the conclusions of this article are available at the NCBI Gene Expression Omnibus repository (http://www.ncbi.nlm.nih.gov/projects/geo/). Level III RNA sequence data of GC are available at UCSC Cancer Browser (https://genome-cancer.ucsc.edu/).

Appendix A. Supplementary data

Supplementary data to this article can be found online at https://doi.org/10.1016/j.neo.2020.09.001.

References

1. Bray F, Ferlay J, Soerjomataram I, Siegel RL, Torre LA, Jemal A. Global cancer statistics 2018: GLOBOCAN estimates of incidence and mortality worldwide for 36 cancers in 185 countries. *CA Cancer J Clin* 2018;**68**:394–424.
2. Siegel RL, Miller KD, Jemal A. Cancer statistics, 2019. *CA Cancer J Clin* 2019;**69**:7–34.
3. Marion RM, Strati K, Li H, Murga M, Blanco R, Ortega S, Fernandez-Capetillo O, Serrano M, Blasco MA. A p53-mediated DNA damage response limits reprogramming to ensure iPS cell genomic integrity. *Nature* 2009;**460**:1149–53.
4. Haapaniemi E, Botla S, Persson J, Schmierer B, Taipale J. CRISPR-Cas9 genome editing induces a p53-mediated DNA damage response. *Nat Med* 2018;**24**:927–30.
5. Rosenfeldt MT, O'Prey J, Morton JP, Nixon C, MacKay G, Mrowinska A, Au TS, Rai TS, Zheng L, Ridgway R, et al. p53 status determines the role of autophagy in pancreatic tumour development. *Nature* 2013;**504**:296–300.
6. Morris JPT, Yashinskie JJ, Koche R, Chandwani R, Tian S, Chen CC, Baslan ZS, Marinkovic ZS, Sanchez-Rivera FJ, Leach SD, et al. alpha-Ketoglutarate links p53 to cell fate during tumour suppression. *Nature* 2019;**573**:595–9.
7. Wang XW, Yeh H, Schaeffer L, Roy R, Moncollin V, Egly JM, Wang Z, Freidberg EC, Evans MK, Taffe BG, et al. p53 modulation of TFIIH-associated nucleotide excision repair activity. *Nat Genet* 1995;**10**:188–95.
8. Jiang L, Kon N, Li T, Wang SJ, Su T, Hibshoosh H, Baer R, Gu W. Ferroptosis as a p53-mediated activity during tumour suppression. *Nature* 2015;**520**:57–62.
9. Aaltonen LA, Peltomaki P, Leach FS, Sistonen P, Pylkkanen L, Mecklin JP, Jarvinen H, Powell SM, Jen J, Hamilton SR, et al. Clues to the pathogenesis of familial colorectal cancer. *Science* 1993;**260**:812–6.
10. Liu Y, Chen C, Xu Z, Scuoppo C, Rillahan CD, Gao J, Spitzer B, Bosbach B, Kastenhuber ER, Baslan T, et al. Deletions linked to TP53 loss drive cancer through p53-independent mechanisms. *Nature* 2016;**531**:471–5.
11. Kern SE, Kinzler KW, Bruskin A, Jarosz D, Friedman P, Prives C, Vogelstein B. Identification of p53 as a sequence-specific DNA-binding protein. *Science* 1991;**252**:1708–11.
12. Dierks C, Grbic J, Zirlik K, Beigi R, Englund NP, Guo GR, Veelken H, Engelhardt M, Mertelsmann R, Kelleher JF, et al. Essential role of stromally induced hedgehog signaling in B-cell malignancies. *Nat Med* 2007;**13**:944–51

13. Sebaa A, Ades L, Baran-Marzack F, Mozziconacci MJ, Penther D, Dobbelstein A, Stamatoullas A, Recher C, Prebet T, Moulessehoul S, et al. Incidence of 17p deletions and TP53 mutation in myelodysplastic syndrome and acute myeloid leukemia with 5q deletion. *Genes Chromosomes Cancer* 2012;**51**:1086–92.
14. Sudmant PH, Mallick S, Nelson BJ, Hormozdiari F, Krumm N, Huddleston J, Coe BP, Baker C, Nordenfelt S, Bamshad M, et al. Global diversity, population stratification, and selection of human copy-number variation. *Science* 2015;**349**:aab3761.
15. Sendoel A, Kohler I, Fellmann C, Lowe SW, Hengartner MO. HIF-1 antagonizes p53-mediated apoptosis through a secreted neuronal tyrosinase. *Nature* 2010;**465**:577–83.
16. Ding L, Lu Z, Lu Q, Chen YH. The claudin family of proteins in human malignancy: a clinical perspective. *Cancer Manage Res* 2013;**5**:367–75.
17. Wu Z, Shi J, Song Y, Zhao J, Sun J, Chen X, Gao P, Wang Z. Claudin-7 (CLDN7) is overexpressed in gastric cancer and promotes gastric cancer cell proliferation, invasion and maintains mesenchymal state. *Neoplasma* 2018;**65**:349–59.
18. Zavala-Zendejas VE, Torres-Martinez AC, Salas-Morales B, Fortoul TI, Montano LF, Rendon-Huerta EP. Claudin-6, 7, or 9 overexpression in the human gastric adenocarcinoma cell line AGS increases its invasiveness, migration, and proliferation rate. *Cancer Invest* 2011;**29**:1–11.
19. Wang K, Li T, Xu C, Ding Y, Li W, Ding L. Claudin-7 downregulation induces metastasis and invasion in colorectal cancer via the promotion of epithelial-mesenchymal transition. *Biochem Biophys Res Commun* 2019;**508**:797–804.
20. Bhat AA, Pope JL, Smith JJ, Ahmad R, Chen X, Washington MK, Beauchamp AB, Singh AB, Dhawan P. Claudin-7 expression induces mesenchymal to epithelial transformation (MET) to inhibit colon tumorigenesis. *Oncogene* 2015;**34**:4570–80.
21. Li W, Xu C, Wang K, Ding Y, Ding L. Non-tight junction-related function of claudin-7 in interacting with integrinbeta1 to suppress colorectal cancer cell proliferation and migration. *Cancer Manage Res* 2019;**11**:1443–51.
22. Ding L, Wang L, Sui L, Zhao H, Xu X, Li T, Wang X, Li W, Zhou P, Kong L. Claudin-7 indirectly regulates the integrin/FAK signaling pathway in human colon cancer tissue. *J Hum Genet* 2016;**61**:711–20.
23. Ding L, Lu Z, Foreman O, Tatum R, Lu Q, Renegar R, Cao J, Chen YH. Inflammation and disruption of the mucosal architecture in claudin-7-deficient mice. *Gastroenterology* 2012;**142**:305–15.
24. Tanaka H, Takechi M, Kiyonari H, Shioi G, Tamura A, Tsukita S. Intestinal deletion of Claudin-7 enhances paracellular organic solute flux and initiates colonic inflammation in mice. *Gut* 2015;**64**:1529–38.
25. Knight JF, Lesurf R, Zhao H, Pinnaduwage D, Davis RR, Saleh SM, Zuo D, Naujokas MA, Chughtai N, Herschkowitz JI, et al. Met synergizes with p53 loss to induce mammary tumors that possess features of claudin-low breast cancer. *Proc Natl Acad Sci U S A* 2013;**110**:E1301–1310.
26. Grobner SN, Worst BC, Weischenfeldt J, Buchhalter I, Kleinheinz K, Rudneva VA, Johann PD, Balasubramanian GP, Segura-Wang M, Brabetz S, et al. The landscape of genomic alterations across childhood cancers. *Nature* 2018;**555**:321–7.
27. Zarrei M, MacDonald JR, Merico D, Scherer SW. A copy number variation map of the human genome. *Nat Rev Genet* 2015;**16**:172–83.
28. Hovhannisyan G, Harutyunyan T, Aroutiounian R, Liehr T. DNA copy number variations as markers of mutagenic impact. *Int J Mol Sci* 2019;**20**.
29. Katoh Y, Katoh M. Comparative integromics on Ephrin family. *Oncol Rep* 2006;**15**:1391–5.
30. Nakayama F, Semba S, Usami Y, Chiba H, Sawada N, Yokozaki H. Hypermethylation-modulated downregulation of claudin-7 expression promotes the progression of colorectal carcinoma. *Pathobiology* 2008;**75**:177–85.
31. Jones PA, Baylin SB. The fundamental role of epigenetic events in cancer. *Nat Rev Genet* 2002;**3**:415–28.
32. Kominsky SL, Argani P, Korz D, Evron E, Raman V, Garrett E, Rein A, Sauter OP, Kallioniemi OP, Sukumar S. Loss of the tight junction protein claudin-7 correlates with histological grade in both ductal carcinoma in situ and invasive ductal carcinoma of the breast. *Oncogene* 2003;**22**:2021–33.
33. Li Y, Gong Y, Ning X, Peng D, Liu L, He S, Gong K, Zhang C, Li X, Zhou L. Downregulation of CLDN7 due to promoter hypermethylation is associated with human clear cell renal cell carcinoma progression and poor prognosis. *J Exp Clin Cancer Res* 2018;**37**:276.
34. Pascal LE, Wang Y, Zhong M, Wang D, Chakka AB, Yang Z, Li F, Song Q, Rigatti LH, Chaparala S, et al. EAF2 and p53 co-regulate STAT3 activation in prostate cancer. *Neoplasia* 2018;**20**:351–63.